Raman scattering in Ti_2O_3-V_2O_3 alloys*

S. H. Shin,† R. L. Aggarwal, and B. Lax‡
Francis Bitter National Magnet Laboratory,§ Massachusetts Institute of Technology, Cambridge, Massachusetts 02139

J. M. Honig
Department of Chemistry, Purdue University, Lafayette, Indiana 47907

(Received 18 July 1973)

Raman scattering of single crystals of $(Ti_{1-x}V_x)_2O_3$ with $0 \leq x \leq 0.3$ has been measured between 80 and 700 °K. All seven Raman-active phonons of the D_{3d}^6 space-group symmetry were found to show appreciable changes in the frequency, linewidth, and relative intensity as a function of temperature and alloy composition in the vicinity of the semiconductor-to-metal transition. In particular, a marked anomaly was observed in the temperature behavior of the lowest frequency mode of A_{1g} symmetry. For $x \lesssim 0.04$ it shows an initial softening followed by a partial recovery in going through the transition temperature. Chi and Sladek have observed a similar decrease and partial recovery for the sound velocity in Ti_2O_3. A qualitative discussion of some of these results is given in terms of the free-energy band-crossing model of Zeiger and co-workers.

I. INTRODUCTION

Titanium sesquioxide Ti_2O_3, which crystalizes in the corundum structure, exhibits pronounced changes in a number of its physical properties in the temperature range ~ 400–550 °K. In particular, resistivity, paramagnetic susceptibility, lattice parameters, and thermoelectric-power measurements by Pearson[1] on sintered samples of Ti_2O_3 and the Hall effect and resistivity measurements of Yahia and Frederikse[2] on presumably single crystals of Ti_2O_3 established that the material undergoes a semiconductor-to-metal transition around 450 °K. Since then a number of investigators[3–10] have studied this transition in pure Ti_2O_3 as well as in its alloys with V_2O_3 $(Ti_{1-x}V_x)_2O_3$, using high-purity single crystals and/or other techniques. For example Rao *et al.*[4] have measured the lattice parameters c and a of pure Ti_2O_3 as a function of temperature and of the alloys at room temperature. In pure Ti_2O_3 they observed very sharp changes in the temperature range 400–470 °K. In the alloys marked changes were observed in the c parameter up to $x = 0.2$, and in the a parameter up to $x \simeq 0.5$. These measurements of the lattice parameters for the alloys at room temperature show that with $x \lesssim 0.1$, the c and a parameters vary with x in the same manner as these parameters vary with temperature in pure Ti_2O_3. For $x \simeq 0.1$, the parameters at room temperature are virtually identical with those of pure Ti_2O_3 above the transition temperature.

Chandrashekhar *et al.*[6] have studied the electrical transition in the alloys. They observed that changes in electrical resistivity of alloys with $x \leq 0.04$ occur in exactly the same temperature range as those in pure Ti_2O_3. Alloys with higher values of x up to 0.10 do not undergo any transition and exhibit metallic behavior over the temperature range between 77 and 600 °K of their experiment.

Recently thermoelectric-power measurements in these alloys have been carried out.[8] For $T > 350$ °K the Seebeck coefficient α for pure Ti_2O_3 diminished rapidly with increasing T, which reflects the semiconductor-to-metal transition. The effect of vanadium doping is found to parallel closely the effects encountered in resistivity measurements. Barros *et al.*[11] have observed an anomaly in the specific heat of single crystals of $(Ti_{1-x}V_x)_2O_3$ with $0 \leq x \leq 0.04$ in the vicinity of the electrical transition. This anomaly was found to vanish at $x = 0.04$.

In this paper we report the Raman investigation of phonons in pure and V-doped Ti_2O_3 for $x \lesssim 0.3$. We have conclusively established the symmetry assignments of all the Raman-active modes. Furthermore, we have made a careful study of the temperature dependence of the phonon frequencies. Temperature effects on Raman scattering in pure Ti_2O_3 were previously reported by Mooradian and Raccah.[7] Considerable softening of all the seven Raman-active phonons was observed in the region of the transition temperature. In the present work we have observed a marked anomaly in the temperature behavior of the lowest-frequency A_{1g} mode. In particular, this mode in pure and V-doped Ti_2O_3 with $x \lesssim 0.04$ shows an initial softening followed by a partial recovery in going through the transition. Chi and Sladek[9] have observed similar softening and partial recovery for the sound velocity in Ti_2O_3. These results are interpreted in terms of the free-energy band-crossing model of Zeiger *et al.*[12] for pure Ti_2O_3.

II. EXPERIMENTAL PROCEDURE

Single crystals of Ti_2O_3-V_2O_3 alloys were grown by the Czochralski-Kyropoulos technique in an

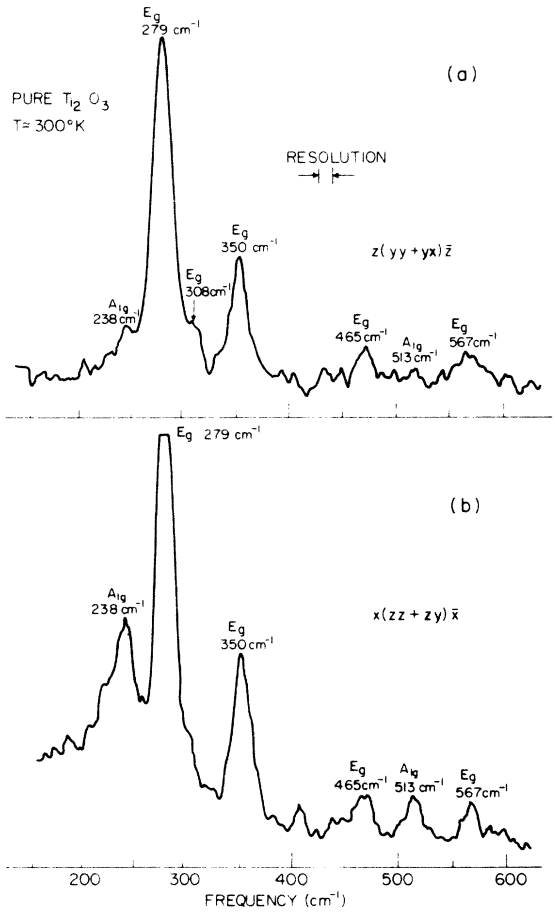

FIG. 1. Stokes Raman spectra of pure Ti_2O_3 at $T \simeq 300$ °K excited with 4880-Å radiation of an argon-ion laser.

electrically heated resistance furnace. Ti_2O_3 samples were prepared by melting stoichiometric portions of Ti metal (99.995%) and TiO_2 (99.99%, major impurities; Fe, 3 ppm; Si, 8 ppm; and Mg, 1 ppm). The alloys were prepared by adding calculated amounts of stoichiometric V_2O_3 obtained by hydrogen reduction from V_2O_5 (99.945%, major impurities; Si, 3 ppm; Mg, 7 ppm). Details of the crystal-growing method are described elsewhere.[13] After x-ray orientation, single-crystal boules were cut into rectangular parallelepipeds approximately $2\times5\times10$ mm in dimension. The specimens were lapped and polished mechanically with 0.05-μ alumina powder.

Raman spectra in the back-scattering configuration were obtained mostly using the 4880-Å excitation line of an argon-ion laser. Other excitation lines of the argon-ion laser were also used in some cases. The experimental setup is essentially the same as that described previously.[14] All the spectra were recorded with 300-μm slits using an integration time of 3 sec on the lock-in amplifier. The low-temperature measurements at ~ 80 °K were made with the specimen in contact with the cold finger of a liquid-nitrogen Dewar. Measurements at and above 300 °K were made using an evacuated high-temperature cell.[15] The sample temperature was monitored by a chromel-constantan thermocouple pressed against the sample surface with a platinum-plus stainless-steel shaving blade.

III. EXPERIMENTAL RESULTS AND DISCUSSION

A. Pure Ti_2O_3

Figure 1 shows some typical Stokes-Raman spectra in pure Ti_2O_3 at room temperature. These spectra were excited with ~ 250-mW power at 4880 Å. The scattering geometry is indicated in Fig. 1 using Porto's[16] notation $\vec{k}_i(e_i e_s)\vec{k}_s$, where $\vec{k}_i$ and $\vec{k}_s$ are the propagation directions of the incident and scattered light, respectively; e_i and e_s in the parentheses are the polarization of the incident and scattered light. The coordinate axes x, y and z used in Fig. 1 and elsewhere in this paper refer to the binary (a), bisectrix (b), and trigonal (c) axes, respectively. As can be seen, the spectra of Fig. 1 show all seven Raman-active phonons allowed in the D_{3d}^6 space-group symmetry of the corundum structure for Ti_2O_3.[17,18] Two of these seven phonons belong to the totally symmetric modes of A_{1g} symmetry and the remaining five phonons belong to the doubly degenerate modes of E_g symmetry. The symmetry assignments as shown in Fig. 1 were determined and confirmed by several polarization experiments. It should be pointed out that the intensity of the A_{1g} modes is considerably higher in the scattering configuration of Fig. 1(b) in comparison to that of Fig. 1(a). For this reason the scattering geometry of Fig. 1(b) was chosen for a determination of the symmetry assignments. This geometry is also to be preferred since optical activity along the trigonal axis could cause a problem in the polarization selection rules.

When the spectra of Fig. 1(b) are analyzed with a polarizer oriented either parallel or perpendicular to the polarization of the incident radiation, results as shown in Fig. 2 were obtained. According to the Raman tensor[19] for the point group D_{3d}, only E_g modes should be observed in the $x(zy)\bar{x}$ spectrum of Fig. 2(b) and only A_{1g} modes should be observed in the $x(zz)\bar{x}$ spectrum of Fig. 2(a). Consistent with this prediction, the spectrum of Fig. 2(b) shows five peaks which are identified with the E_g symmetry. Similarly the two peaks at 238 and 513 cm^{-1} in Fig. 2(a) are identified with the A_{1g} symmetry. We believe that the peak at 279 cm^{-1} in Fig. 2(a) is due to the strongest E_g mode [see Fig. 2(b)] and is observed due to incomplete polarization generally character-

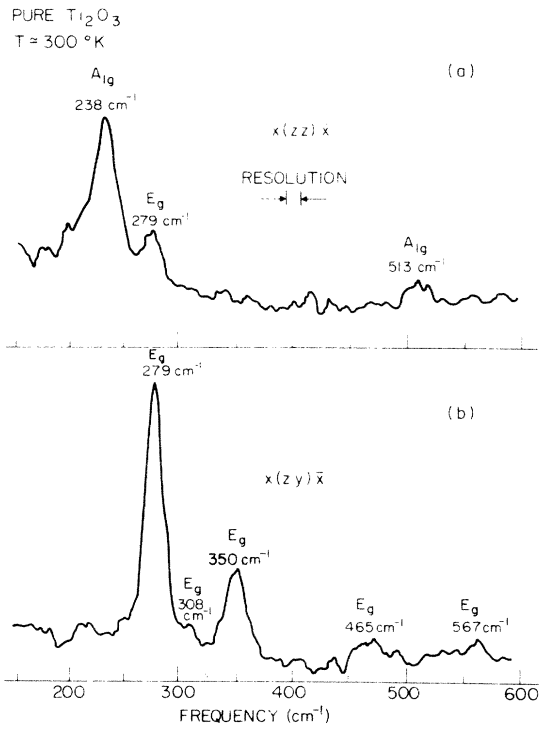

FIG. 2. Polarization spectra of pure Ti_2O_3.

istic of back-scattering measurements. Thus if the seven Raman-active phonons of Ti_2O_3 are labeled 1–7 in order of increasing frequency, we conclude that the modes 1 and 6 have A_{1g} symmetry and the remaining five modes have E_g symmetry. This symmetry assignment is different from that reported previously by Mooradian and Raccah[7] in that they identified modes 1 and 2 as of E_g and A_{1g} symmetry, respectively. We believe that their symmetry assignment of modes 1 and 2 was in error. A number of other observations, discussed later, corroborate our symmetry assignment. Except for this discrepancy in symmetry assignment, our spectra of pure Ti_2O_3 are in good agreement with those of Ref. 7, as may be seen in Table I.

The temperature dependence of the frequencies of all the Raman-active modes for pure Ti_2O_3 is shown in Fig. 3. The observed temperature softening is generally consistent with that reported in Ref. 7. However, there are some differences in the two measurements. For example, we observe a decrease in frequency of 44 cm^{-1} between 300 and 600 °K for the lowest-frequency E_g mode, as compared with that of 31 cm^{-1} in Ref. 7 for the same temperature range. Furthermore, most of the softening observed by us occurred in a smaller temperature interval. Both these features suggest that our samples may be of higher purity as inferred from the trends found in the doped crystals.

Another very interesting feature shown in Fig. 3 is the behavior of the lowest-frequency A_{1g} mode. It exhibits a decrease in frequency of ~ 14% up to ~ 450 °K and then an increase of ~ 6% between 450 and 700 °K. This frequency softening followed by a partial recovery for the A_{1g} mode had been predicted theoretically by Zeiger *et al.*[12] based on the free-energy band-crossing model of Ti_2O_3. This model is based on a two-band Hubbard model including both the electron-electron Coulomb and lattice-displacement energies. The Helmholtz free energy of the system can be written in the form[12]

$$F(\delta, r, \tau) = \delta^2/2\kappa + \tfrac{1}{2}ur^2 - (\tau/2N)\left[\int \rho_2(\epsilon)\ln(1+e^{(\mu-\epsilon)/\tau})d\epsilon + \int \rho_1(\epsilon)\ln(1+e^{-(\mu+\epsilon+\Delta)/\tau})d\epsilon\right], \quad (1)$$

where the first term on the right-hand side is the electron-Coulomb-repulsion energy, the second term is the lattice-displacement energy, and the third term is the energy due to the electron and hole entropy. Here δ is proportional to the number of electrons in the conduction band, μ is the Fermi energy, and r is the lattice-displacement parameter. $\rho_1(\epsilon)$ and $\rho_2(\epsilon)$ are the densities of electron states in valence and conduction bands, respectively, and N is the number of unit cells. τ and ϵ are, respectively, temperature and energy variables normalized to the energy gap at $T = 0$. Δ is the normalized energy gap given by

$$\Delta = 1 - \delta - er + vr^2, \quad (2)$$

where e, v, and u are fixed parameters, whereas κ is an adjustable parameter of the model. The conservation of the number of electrons in an intrinsic semiconductor and the equilibrium condition yield the following equations:

TABLE I. A summary of frequencies and symmetry assignments of Raman-active phonons in pure Ti_2O_3 at $T \simeq 300$ °K.

Mode No.	Symmetry	Frequency (cm^{-1}) this work	Ref. 7
1	A_{1g}	238	228
2	E_g	279	274
3	E_g	308	302
4	E_g	350	347
5	E_g	465	452
6	A_{1g}	513	530
7	E_g	567	564

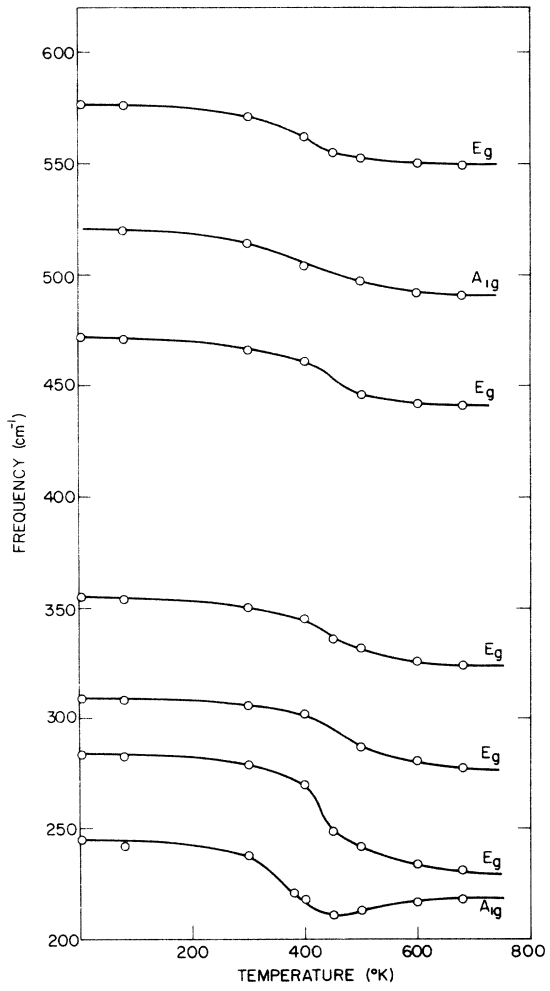

FIG. 3. Phonon frequency vs temperature for Raman-active modes of Ti_2O_3.

$$\int \frac{\rho_2(\epsilon)}{1+e^{(\mu-\epsilon)/\tau}}\,d\epsilon = \int \frac{\rho_1(\epsilon)}{1+e^{-(\mu+\epsilon+\Delta)/\tau}}\,d\epsilon, \tag{3}$$

$$\delta = \kappa\,\langle n_2\rangle/2N, \tag{4}$$

$$r = (e\delta/\kappa u)\,(1+2v\delta/\kappa u)^{-1}. \tag{5}$$

Here $\langle n_2\rangle$ is the number of electrons in the conduction band. Equations (3)–(5) indicate that the lattice parameter is governed by the electron density of the conduction band.

It is assumed that the force constant associated with c-axis motion is proportional to d^2F/dr^2, and therefore a phonon mode dominated by c-axis motion has a Raman frequency

$$\omega_R \propto \left(\frac{d^2F}{dr^2}\right)^{1/2}, \tag{6}$$

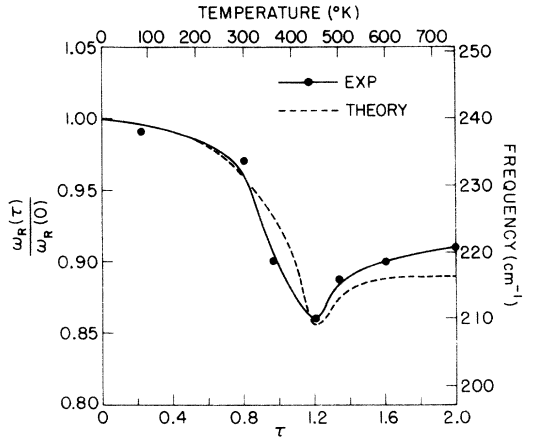

FIG. 4. Comparison of experiment and theory for the temperature dependence of the lowest-frequency A_{1g} mode in Ti_2O_3. The dimensionless variable τ along the lower abscissa is the temperature normalized to the energy gap at $T=0$.

where

$$\frac{d^2F}{dr^2} = \frac{\partial^2F}{\partial r^2} + \frac{\partial}{\partial\mu}\left(\frac{\partial F}{\partial r}\right)\frac{d\mu}{dr} + \frac{\partial}{\partial\delta}\,\frac{\partial F}{\partial r}\,\frac{d\delta}{dr}. \tag{7}$$

For given values of e, v, u and κ, d^2F/dr^2 is evaluated numerically as follows. At first one obtains equilibrium values of r, μ, and δ by using the equilibrium conditions

$$\left(\frac{\partial F}{\partial r}\right) = \frac{\partial F}{\partial\mu} = \frac{\partial F}{\partial\delta} = 0.$$

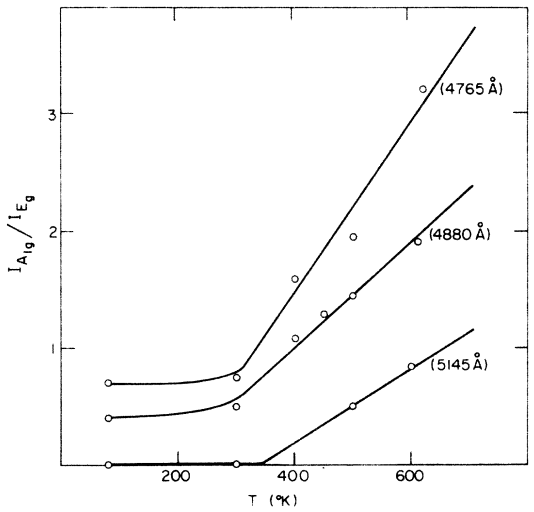

FIG. 5. Ratio of the peak intensities of the lowest-frequency A_{1g} mode and its adjacent E_g mode vs temperature.

Then one allows a small change Δr under the quasi-equilibrium condition $\partial F/\partial \mu = \partial F/\partial \delta = 0$. Taking $\partial F/\partial r$ equal to a small value Q, one can calculate the corresponding Δr, and d^2F/dr^2. In Fig. 4 we compare the observed frequency change of the lowest-frequency A_{1g} mode versus T with the above theoretical model. The theoretical curve shown in Fig. 4 which provided the best fit to our experimental data was calculated by Zeiger[20] using the following values for the model parameters: $\kappa = 10.0$, $u = 330$, $v = 33$, $e = 7.25$, the valence bandwidth $b_1 = 10$, and the conduction bandwidth $b_2 = 3$. As can be seen in Fig. 4, a fairly good agreement is obtained between experiment and theory.

Another interesting feature of the Raman scattering in Ti_2O_3 is the temperature enhancement of the scattering intensity of the A_{1g} modes relative to that of the E_g modes, as first reported by Mooradian and Raccah.[7] Our results for the lowest-frequency A_{1g} and E_g modes are shown in Fig. 5, and were obtained with excitation lines at 5145 (2.41 eV), 4880 (2.54 eV), and 4765 Å (2.60 eV). As seen in Fig. 5, the temperature enhancement is most pronounced in spectra obtained with 4765-Å (2.60-eV) radiation. This frequency dependence of the temperature enhancement is similar to the laser excitation frequency dependence of the A_{1g} mode observed at room temperature. As pointed out in Ref. 7, it may be due to an energy gap of 2.8 eV deduced by Scouler and Raccah[21] from reflectivity measurements.

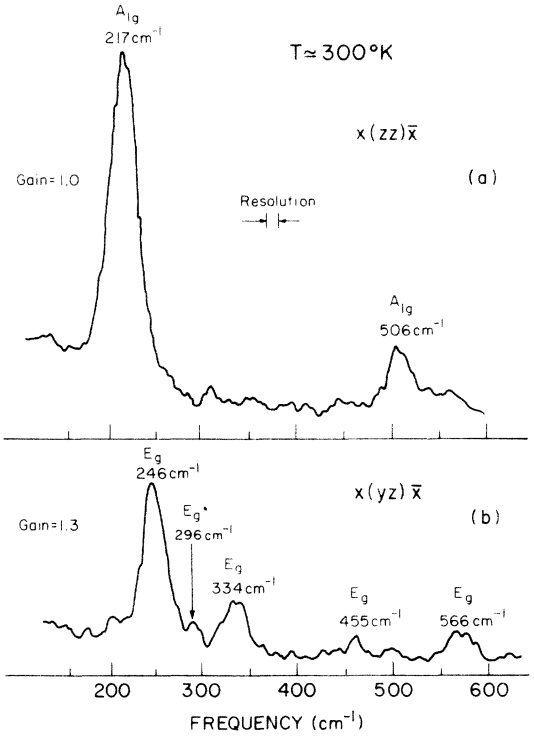

FIG. 6. Polarization spectra of $(Ti_{1-x}V_x)_2O_3$ with $x = 0.08$.

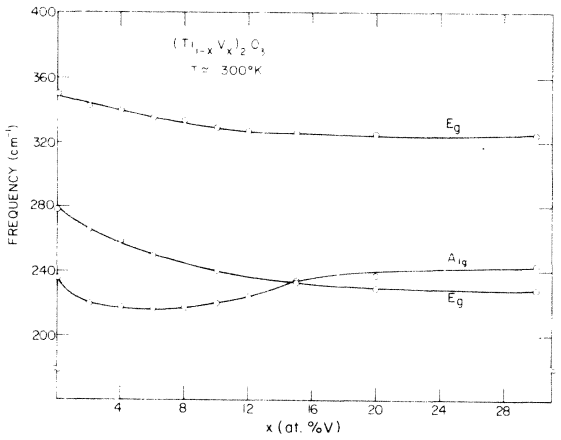

FIG. 7. Phonon frequencies vs vanadium doping (x) in $(Ti_{1-x}V_x)_2O_3$ at $T \simeq 300$ °K.

B. V-doped $Ti_2O_3(Ti_{1-x}V_x)_2O_3$

It is known that the incorporation of V_2O_3 into Ti_2O_3 causes an increase in the c/a ratio of the lattice parameters for the rhombohedral unit cell[22,23] and drastically changes its electrical characteristics.[6,8] A measurement of the lattice parameters of mixed crystals at room temperature shows that the parameters c and a vary with x in the same manner as those of pure Ti_2O_3 vary with temperature for $x \lesssim 0.1$.

We have observed an analogous effect in the Raman scattering of $(Ti_{1-x}V_x)_2O_3$, i.e., phonon frequencies in the mixed crystals show changes with vanadium concentration in a way which is essentially similar to the temperature-induced changes in the phonon frequencies of pure Ti_2O_3. A typical set of Stokes-Raman lines for an 8.0-at.% V specimen are shown in Fig. 6. The top spectrum is for the $x(zz)\bar{x}$ scattering geometry and the bottom spectrum corresponds to the $x(zy)\bar{x}$ configuration. A comparison of these spectra to those given in Fig. 2 for pure Ti_2O_3 shows that there is no change in the symmetry ordering. However, the frequencies of all the seven Raman modes in the doped crystal are lower than those of pure Ti_2O_3. In addition, the scattering intensity of the A_{1g} modes normalized to (say) the lowest-frequency E_g mode is higher in the doped crystal than that in the pure crystal. These changes in the scattering intensity with V doping are also similar to those observed in pure Ti_2O_3 temperature

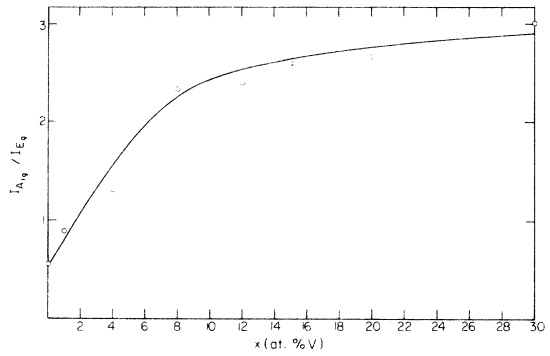

FIG. 8. Ratio of the peak intensities of the lowest-frequency A_{1g} mode and its adjacent E_g mode vs vanadium doping (x) in $(Ti_{1-x}V_x)_2O_3$ at $T \simeq 300$ °K.

(see Fig. 5).

Shown in Fig. 7 are the phonon frequencies vs vanadium concentration for the lowest-frequency A_{1g} mode and for the two strongest E_g modes at room temperature. In the case of E_g modes the frequency decreases with x up to 0.3 which is the highest doping concentration studied in this work. The frequency of the A_{1g} mode shows quite a different behavior as a function of x. It shows a marked softening in the range $0 \leq x \leq 0.04$ and very small changes in the region $0.04 \leq x \leq 0.1$. For > 0.1 the frequency of the A_{1g} mode exhibits an increase with increasing x. At $x \simeq 0.15$ the frequencies of the lowest A_{1g} and E_g modes become equal. For still larger values of x, the frequency of the A_{1g} mode becomes higher than that of the E_g mode. Thus for $x > 0.15$, the summetry ordering of the Raman modes becomes the same as that observed in other isomorphic crystals such as Al_2O_3 [16] and Cr_2O_3. [24] Thus one may expect the Raman-active phonons in pure V_2O_3 ($x = 1$) to have the same symmetry ordering as in these other isomorphic materials. The frequency softening up to 10-at.%-V-doped Ti_2O_3 is clearly associated with the semiconductor-to-metal transition, which is consistent with the change in the c parameter for V-doped samples at 300 °K. The frequency recovery in samples with $x > 0.1$ corresponds to the range above the transition temperature for pure Ti_2O_3. As indicated earlier in Sec. I, it has been demonstrated that the crystallographic parameters of 10-at.%-V-doped Ti_2O_3 at 300 °K are virtually identical with those for pure Ti_2O_3 above the transition range. Furthermore, this mixed crystal does not undergo a transition.

In addition to the above changes in the phonon frequencies with vanadium doping in Ti_2O_3, we have also observed appreciable enhancement in the

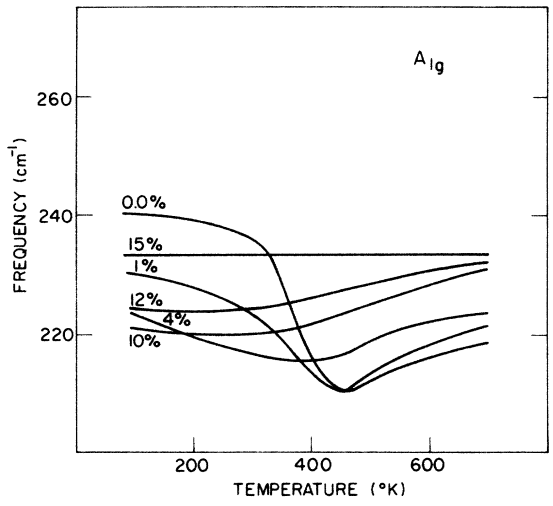

FIG. 9. Phonon frequency vs temperature for the lowest-frequency A_{1g} mode in $(Ti_{1-x}V_x)_2O_3$ for several values of x given in at.%.

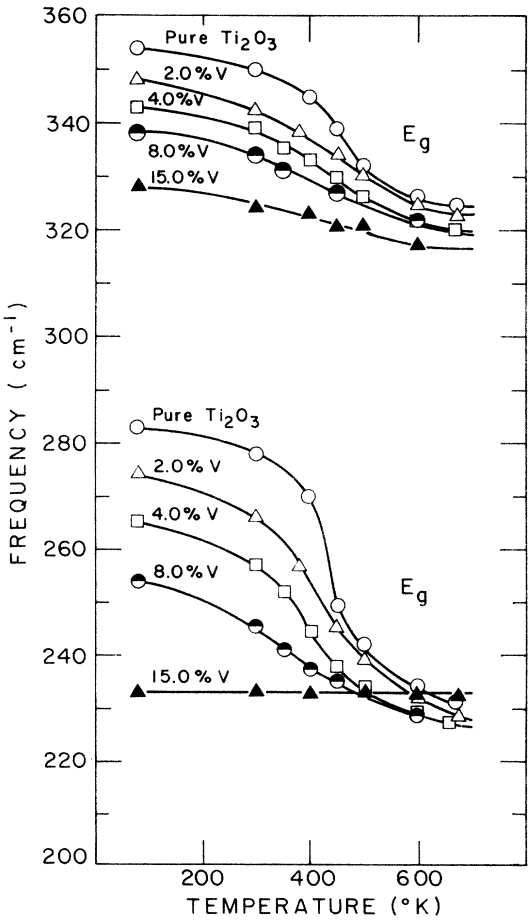

FIG. 10. Phonon frequency vs temperature for the two strongest E_g modes in $(Ti_{1-x}V_x)_2O_3$ for several values of x given in at.%.

scattering intensity of the A_{1g} modes relative to that of the E_g modes with the addition of vanadium. This is illustrated in Fig. 8 which shows the peak intensity of the lowest-frequency A_{1g} mode relative to that of the low-frequency E_g mode. This intensity enhancement is most pronounced for $x \leq 0.1$. Though we have not considered a model to explain the observed intensity enhancement even qualitatively, it is worth noting that the shape of the enhancement curve of Fig. 8 bears a close resemblance to the curves for the lattice parameters vs x for $0 \leq x \leq 0.3$.[23]

The temperature dependence of the frequency of the A_{1g} mode in mixed crystals is shown in Fig. 9 from 80 to 700 °K. For $0 \leq x \leq 0.04$ the frequency undergoes marked softening and subsequent recovery in the vicinity of the transition. This frequency anomaly is found to be smaller the larger the V content and disappears for $x > 0.04$. At least qualitatively this anomalous behavior can be understood in the framework of Zeiger's band-crossing free-energy model by considering that a few percent addition of V into Ti_2O_3 is equivalent to a few percent decrease in the parameter κ.[20] Samples with $0.04 < x < 0.15$ exhibit only an increase in frequency over the entire temperature range of this work and no frequency change was observed in the 15-at.%-V sample in which both A_{1g} and E_g modes are superimposed at room temperature. These results are consistent with the resistivity measurements which show that the electrical transition becomes less and less pronounced as V doping is increased. In fact, the electrical transition disappears for the material with $x > 0.04$ having metallic behavior at all temperatures. It is also worth pointing out that the specific-heat anomaly observed in the vicinity of the electrical transition by Barros *et al.*[11] becomes smaller with the increase in V-doping and vanishes for $x = 0.04$.

The temperature behavior of the frequency for two of the strongest E_g modes in mixed crystals is shown in Fig. 10. In contrast to the A_{1g} modes, E_g modes do not show any frequency recovery on going through the transition temperature. It is found that with increased V doping in Ti_2O_3, all the curves nearly merge smoothly with the curve of pure Ti_2O_3 above the transition temperature. This characteristic difference between modes of different symmetry shows that the A_{1g} mode is an excellent indicator of the electrical behavior of Ti_2O_3 with temperature as well as V doping.

IV. CONCLUSIONS

In conclusion we have established the symmetry assignments of the seven Raman-active modes in $(Ti_{1-x}V_x)_2O_3$ with $x \leq 0.3$. A marked anomaly observed in the frequency of the A_{1g} mode with temperature is found to be in agreement, at least, qualitatively, with the free-energy-band crossing model of Zeiger and co-workers.

ACKNOWLEDGMENTS

The authors are grateful to Dr. H. J. Zeiger for many stimulating discussions on the subject and for providing us the results of his calculations prior to publication. They are also grateful to Professor P. M. Raccah for several discussions on the phonon-symmetry assignments, and in particular, for his help in repeating some of the experiments at the Yeshiva University. They are pleased to acknowledge the help of G. Yuochunas and Dr. G. V. Chandrashekhar in the crystal growth. They also wish to thank Dr. J. C. Tsang for his help during the measurements and L. V. Sousa for assistance with crystal polishing.

---

*Part of this work was supported on the Advanced Research Projects Agency-IDL grant to Purdue University.

†Visiting graduate student from Purdue University. Present address: Dept. of Physics, Yeshiva University, New York, N. Y. 10033.

‡Also, Physics Dept., Massachusetts Institute of Technology.

§Supported by the National Science Foundation.

[1]A. D. Pearson, J. Phys. Chem. Solids 5, 316 (1958).

[2]J. Yahia and H. P. R. Frederikse, Phys. Rev. 123, 1257 (1961).

[3]S. Nomura, T. Kawakubo, and T. Yanagi, J. Phys. Soc. Jap. 16, 706 (1961).

[4]C. N. Rao, R. E. Loehman, and J. M. Honig, Phys. Lett. A 27, 271 (1968).

[5]J. M. Honig and T. B. Reed, Phys. Rev. 174, 1020 (1968).

[6]G. V. Chandrashekhar, Q. Won Choi, J. Moyo, and J. M. Honig, Mater. Res. Bull. 5, 999 (1970).

[7]A. Mooradian and P. M. Raccah, Phys. Rev. B 3, 4253 (1971).

[8]S. H. Shin, G. V. Chandrashekhar, R. E. Loehman, and J. M. Honig, Phys. Rev. B 8, 1364 (1973).

[9]T. C. Chi and R. J. Sladek, Phys. Rev. B 7, 5080 (1973).

[10]M. E. Sjöstrand and P. H. Keesom, Phys. Rev. B 7, 3558 (1973).

[11]H. L. C. Barros, G. V. Chandrashekhar, T. C. Chi, J. M. Honig, and R. J. Sladek, Phys. Rev. B 7, 5147 (1973).

[12]H. J. Zeiger, T. A. Kaplan, and P. M. Raccah, Phys. Rev. Lett. 26, 1328 (1971).

[13]T. B. Reed, R. E. Fahey, and J. M. Honig, Mater. Res. Bull. 2, 561 (1967).

[14]R. K. Ray, R. L. Aggarwal, and B. Lax, in *Proceedings of the Second International Conference on Light Scattering in Solids, Paris*, 1971 (Flammarion, Paris, 1971), p. 288.

[15]T. R. Hart, Ph. D. thesis (M. I. T., 1970) (unpub-

lished).
[16]S. P. S. Porto and R. S. Krishman, J. Chem. Phys. 47, 1009 (1967).
[17]R. W. G. Wyckoff, *Crystal Structure* (Interscience, New York, 1951), Chap. V.
[18]S. Bhagavantam and T. Venkalarayadu, Proc. Ind. Acad. Sci. A 10, 224 (1938).
[19]R. Loudon, Adv. Phys. 13, 423 (1964).
[20]H. J. Zeiger, Bull. Am. Phys. Soc. 18, 399 (1973); it should be pointed out this curve was obtained from his preliminary calculations only and is presented here for the purpose of a qualitative comparison with our data.
[21]W. J. Scouler and P. M. Raccah, Bull. Am. Phys. Soc. 15, 289 (1970).
[22]T. Kawakubo, T. Yanagi, and S. Nomura, J. Phys. Soc. Jap. 15, 2102 (1960).
[23]R. E. Loehman, C. N. R. Rao, and J. M. Honig, J. Phys. Chem. 73, 1781 (1969).
[24]T. R. Hart, R. L. Aggarwal, and B. Lax, in Ref. 14, p. 174.